Wavelength and power dependence on multilevel behavior of phase change materials

Cite as: AIP Advances **11**, 085327 (2021); https://doi.org/10.1063/5.0058178
Submitted: 01 June 2021 • Accepted: 08 August 2021 • Published Online: 24 August 2021

Gary A. Sevison, Joshua A. Burrow, Haiyun Guo, et al.

Wavelength and power dependence on multilevel behavior of phase change materials

Cite as: AIP Advances 11, 085327 (2021); doi: 10.1063/5.0058178
Submitted: 1 June 2021 • Accepted: 8 August 2021 •
Published Online: 24 August 2021

Gary A. Sevison,[1,2,a] Joshua A. Burrow,[1] Haiyun Guo,[1] Andrew Sarangan,[1] Joshua R. Hendrickson,[2] and Imad Agha[1,3]

AFFILIATIONS

[1] Department of Electro-Optics and Photonics, University of Dayton, Dayton, Ohio 45469, USA
[2] Air Force Research Laboratory, Sensors Directorate, Wright-Patterson Air Force Base, Ohio 45433, USA
[3] Department of Physics, University of Dayton, Dayton, Ohio 45469, USA

[a] Author to whom correspondence should be addressed: sevisong1@udayton.edu

ABSTRACT

We experimentally probe the multilevel response of GeTe, $Ge_2Sb_2Te_5$ (GST), and 4% tungsten-doped GST (W-GST) phase change materials (PCMs) using two wavelengths of light: 1550 nm, which is useful for telecom-applications, and near-infrared 780 nm, which is a standard wavelength for many experiments in atomic and molecular physics. We find that the materials behave differently with the excitation at the different wavelengths and identify useful applications for each material and wavelength. We discuss thickness variation in the thin films used as well and comment on the interaction of the interface between the material and the substrate with regard to the multilevel behavior. Due to the differences in penetration depths, absorption, and index contrast, different PCMs could be more suitably used depending on the application and wavelength of operation.

I. INTRODUCTION

Phase change materials (PCMs), such as Germanium Telluride (GeTe), Germanium Antimony Telluride (GST), and their doped variants have been attracting more and more attention in the field of reconfigurable photonics. Essentially, as the material transitions between its amorphous and crystalline states through either an optically or electrically imparted thermal excitation, that transition is accompanied by a very large change in the refractive index, on the order of 50%, leading to a whole host of potential applications, ranging from optical storage and memories all the way to novel neuromorphic computing protocols and reconfigurable nanophotonics.[1–7] In the field of reconfigurable nanophotonics, there is merit to laser-assisted optical reconfiguration that allows for multifunctional optical elements such as the gratings created by Trofimov *et al.*[8] and other such devices.[9,10]

A big part of the advancement is in the solutions that have been developed recently to problems that have often plagued the material, such as high resistivity,[11,12] high optical losses,[13,14] and material lifetime.[15] The phase space for optimizing PCMs is enormous, making it critical to continue performing fundamental studies on the response of the material to optical and electronic excitation under disparate conditions. Devices based on PCMs could be divided according to whether the devices are actuated optically via a laser pulse[16–18] or electrically via an electronic pulse.[19–24] While electronic excitation is important for applications such as electronic memories, optical modulators, and color displays, optical excitation will equally play an important role in future technologies, such as optical memories, phase plates, optical limiters, to name just a few.

For pulsed optical excitation, which is critical for a wide range of applications as stated above, some of the parameters to investigate are the wavelength of excitation, the temporal pulse shape and duration, sample thickness, and the alloying and doping of the material itself. Ultimately, the goal would be to produce a catalog of materials and their disparate properties (index contrast upon phase change, optical losses, switching speed, and intermediate/multilevel switching).

In this paper, we highlight three types of chalcogenide materials that have shown potential as optical phase change materials:

GST,[1,25,26] W-GST,[12] and GeTe.[27–30] While GST is a ubiquitous phase change material with a multitude of uses, its doped variant shows an altered response due to increased electrical and thermal conductivity,[12] leading to potentially different regimes of application. On the other hand, the GeTe alloy, which exhibits higher temperature threshold for phase transition, exhibits lower losses and consequently higher efficiency for optical modulation. Our results are further proof that multilevel, high speed optical switching and storage are viable technologies for future devices provided that the PCM composition and configuration are well understood and optimized to the optical switching pulse characteristics.

II. EXPERIMENTAL METHODS

The data in this study were gathered from a custom built optical setup that allows for full control of the power, temporal shape, and number of pulses in a laser incident on a thin film of a PCM. For the data at 1550 nm light, we inserted a 1590 nm continuous-wave (CW) laser to the fiber with the pump laser to act as a probe beam. This beam is coupled into the fiber before the beam transitions to free-space in order to simplify the alignment. The 1550 nm pulse train and the 1590 nm CW beam are passed through a microscope objective that focuses the spot down to ~2 μm in diameter, and it hits the sample imparting a phase change of the material; the 1590 nm light is picked up after reflecting off of the sample and input to a balanced detector. The control arm of the balanced detector is taken from a pick off before the beam was focused onto the sample via a microscope. The change in reflectivity is then recorded by a detector and oscilloscope. The pulses used in this investigation were of varying powers but kept at a 50 ns long square pulse with a 25 ns falling shape. This allows for controlled cooling of the material in order to give the material time to crystallize. To generate the 775 nm pulses, we passed the 1550 nm pulsed light through a periodically poled lithium niobate (PPLN) crystal where the light was frequency doubled to obtain the intended wavelength. Care was taken to measure the pulse after the conversion to correct for any non-linear shortening or steepening of the pulse. After the conversion, an 820 nm CW source was co-aligned and co-focused onto the sample to be used as a probe beam. The 820 nm CW beam was then detected by an avalanche photo diode (APD) and recorded by the same oscilloscope as before. A diagram of the setup is shown in Fig. 1. More information about the setup in the 1550 nm configuration can be found in our previous paper.[1]

Three chalcogenide materials were investigated in this experiment. Germanium telluride (GeTe), germanium antimony telluride (GST), and 4% tungsten-doped GST (W-GST) were considered for their phase change abilities and as they were the subject of our recent efforts.[1,12] Each material was subjected to a train of excitation pulses at 775 and 1550 nm to induce crystallization, and their reflectivities were read out in order to determine their use in multilevel free space applications. These experiments were performed initially on samples with thicknesses in the 140–170 nm range. Thicker samples were fabricated via sputtering and measured as well to account for the larger penetration depths as the pump wavelength was increased. These thicker samples ranged from 350 nm for W-GST to 530 nm for GST. The reflectivity plots can be seen in Sec. III. Raman spectroscopy was considered to verify the material switching; however, the spot sizes achieved with our setup are

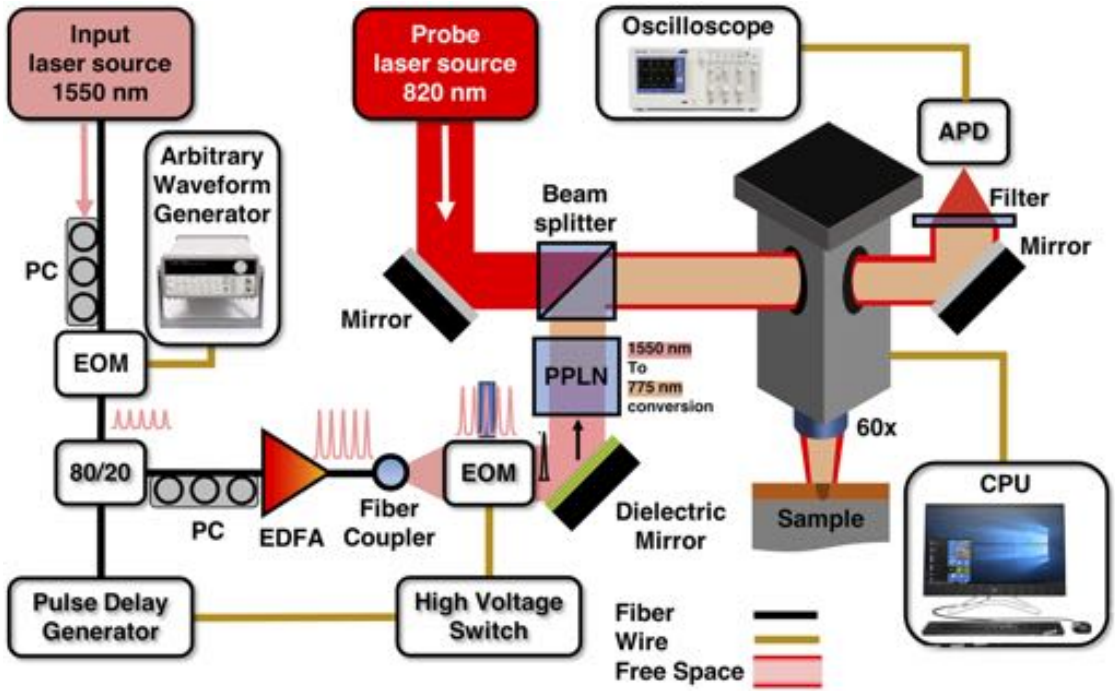

FIG. 1. Experimental setup.

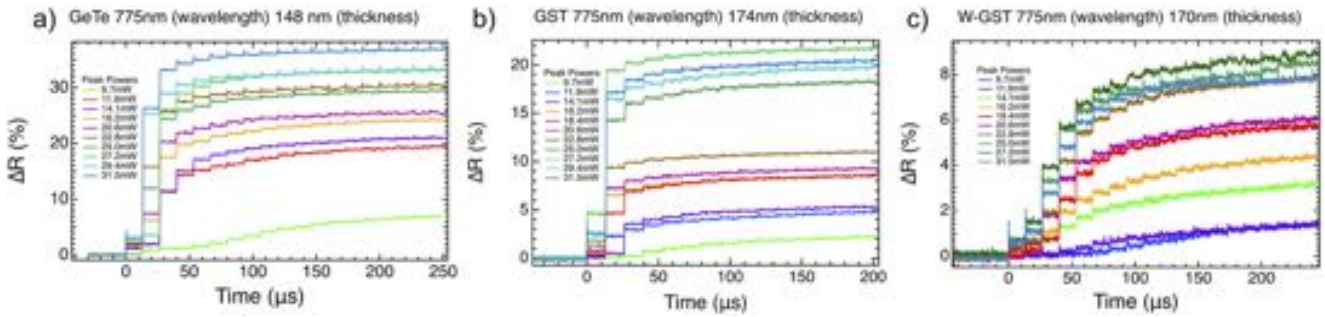

FIG. 2. Multipulse response of (a) GeTe, (b) GST, and (c) W-GST for 775 nm excitation.

too small for our Raman microscope, leading us to utilize a thermal model to explain the partial states seen in the experimental data.

III. RESULTS

Figure 2 shows the 775 nm excitation results on the thin samples. We clearly observe a difference in the reflectivity measurements upon crystallization in each of the samples. GeTe and GST both have a large ΔR compared to W-GST, where ΔR is the total difference between the fully amorphous reflectivity before a single pulse hits the thin film and the final distinguishable reflectivity level of the switched material. However, both GeTe and GST exhibit very pronounced non-linear switching with multiple pulses. After there is a small initial crystallization, as seen after the first pulse in Figs. 2(a) and 2(b), the second pulse usually gives a large jump in reflectivity. We suspect this is due to the thermal transport and absorption of the crystalline state. These materials would be well suited for applications needing high contrast between the two states. On the other hand, W-GST, while having a more linear step size, has fewer accessible levels and is only 20% of the ΔR of GeTe, as can be seen in Table I. The peaks seen at the boundary between some levels in the data can be attributed to the material's reaction to the pulse and its physical switching between states. We have discussed this phenomenon in much greater detail in our previous work.[1]

Moving on to the 1550 nm excitations shown in Fig. 3, we see a change in the behaviors. In this wavelength regime, we can see that the best performer in terms of both linearity and number of levels is GST. We also begin to see interesting behavior in both GeTe and W-GST. In GeTe, we begin to see issues arising from ablation. This can be seen where the graph drops below a previous level or even below the zero point. This is ablation at the center of the illuminated spot. The levels are still able to climb after the ablation since the crystallized portion is spreading horizontally. This is not ideal for a device since the ablated area cannot be switched back and is permanently destroyed. With a low absorption coefficient and a lower index of refraction (as seen in Table I), higher powers are needed in order to achieve crystallization in the thin sample. This causes a larger area to crystallize and therefore gives us fewer levels and a tendency to ablate quickly at these higher powers. To better understand what was occurring in the samples, simulations were carried out in a two-step process via Lumerical HEAT. After the first pulse, the area above the crystallization temperature is treated as crystallized, and a mixed layer of two states is created to receive the second pulse. The thermal properties used in the simulations were taken from three papers.[12,32,33] Figure 4 shows these simulations, and it can be seen that for the second pulse incident on the PCM, there are two hot

TABLE I. Material and multipulse properties of GeTe, GST, and W-GST.

	Amorphous and crystalline $\tilde{n}$		At 775 nm	At 1550 nm (thin)	At 1550 nm (thick)
GeTe	a at 775 nm 3.49 + 0.65i[31] c at 775 nm 5.03 + 1.86i[31] a at 1550 nm 3.26 + 0.04i[31] c at 1550 nm 5.04 + 0.33i[31]	No. of levels Peak power ΔR	12 18.4 mW 23.2%	8 302.3 mW 8.3 a.u.	11 114.9 mW 17.9 a.u.
GST	a at 775 nm 4.49 + 1.37i c at 775 nm 5.46 + 2.46i a at 1550 nm 4.24 + 0.05i c at 1550 nm 6.11 + 0.72i	No. of levels Peak power ΔR	8 25.0 mW 17.5%	13 66.5 mW 19.6 a.u.	8 96.7 mW 9.3 a.u.
W-GST	a at 775 nm 4.43 + 1.44i c at 775 nm 5.10 + 3.52i a at 1550 nm 4.44 + 0.28i c at 1550 nm 6.60 + 1.17i	No. of levels Peak power ΔR	10 16.2 mW 3.5%	10 48.4 mW 4.0 a.u.	9 39.3 mW 6.6 a.u.

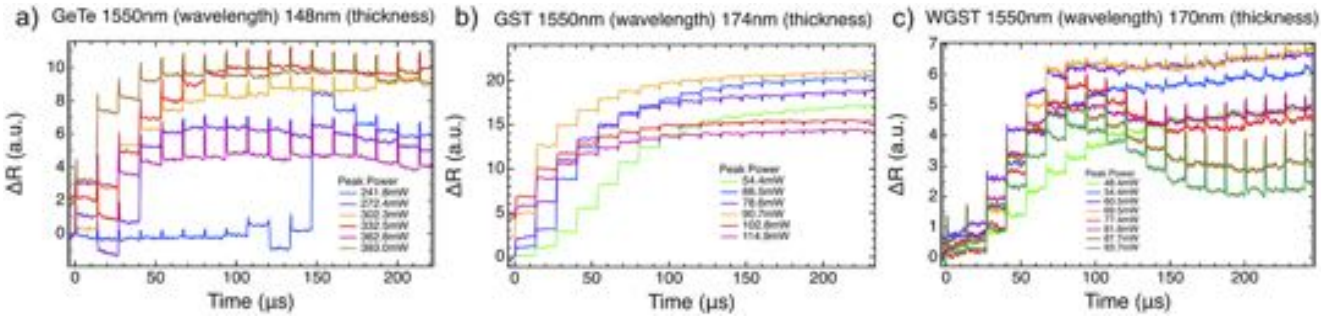

FIG. 3. Multipulse response of (a) GeTe, (b) GST, and (c) W-GST for 1550 nm excitation.

spots on the sides of the crystallized area and for the case of W-GST, a third central hotspot can be seen. This is due to the discontinuity the E-field sees in the index of refraction between the crystalline and the amorphous states of the material where the edge is perpendicular to the polarization of the field. When the polarization is rotated 90° in our 2D simulations the phenomenon is no longer seen. The hot spots are the areas where the ablation can initially occur and cause the drops in reflectivity seen in Fig. 3. In W-GST, we see ablation occurring as well. This reveals itself with the dropping of the levels after the initial climb. W-GST's ablation is much more consistent and can be avoided by using lower powers, as shown in the traces that do not have a turning point where the reflectivity begins to drop. This lower power region is also where we see the largest number of intermediate levels available.

In the third set of trials, we used thicker samples in order to account for the lower material absorption at the longer 1550 nm wavelength used to excite the material. The results are shown in Fig. 5. We noticed that with the smaller spot size, we achieved fewer levels than in our previous work (~2 μm in diameter compared to ~5 μm previously)[1] in GST. We believe this to be due to the smaller volume available for switching. Using similar powers to those previously used, similar sized volumes will be changed in both instances, and this will limit the number of available levels as we drop the accessible volume. Here, we can see that the erratic behavior of the ablation in GeTe has been resolved. We still see ablation occurring at longer wavelengths; however, this is expected as the material is more absorptive in the crystalline state. This can be seen in both GeTe and GST (while we do not perform this measurement on W-GST due to sample availability, we expect the behavior to be broadly similar). In this regime, we begin to see GeTe again having the highest number of levels, and we see the step sizes of the levels moving toward being more linear than the other thicknesses or

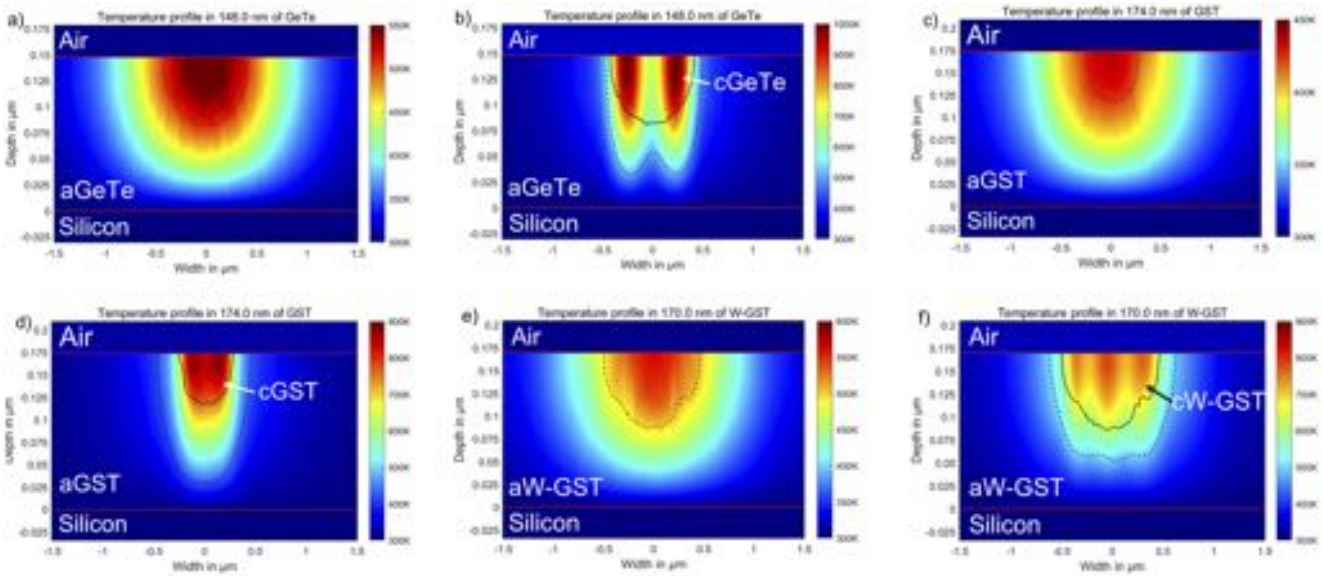

FIG. 4. Lumerical HEAT simulations showing the temperature profile for the first and second pulses from a 1550 nm wavelength Gaussian beam on each of the three thin samples: (a) and (b) GeTe, (c) and (d) GST, and (e) and (f) W-GST. Dotted lines on graphs show the area where crystallization is expected to occur. Solid lines on graphs indicate the area considered crystallized for the second pulse.

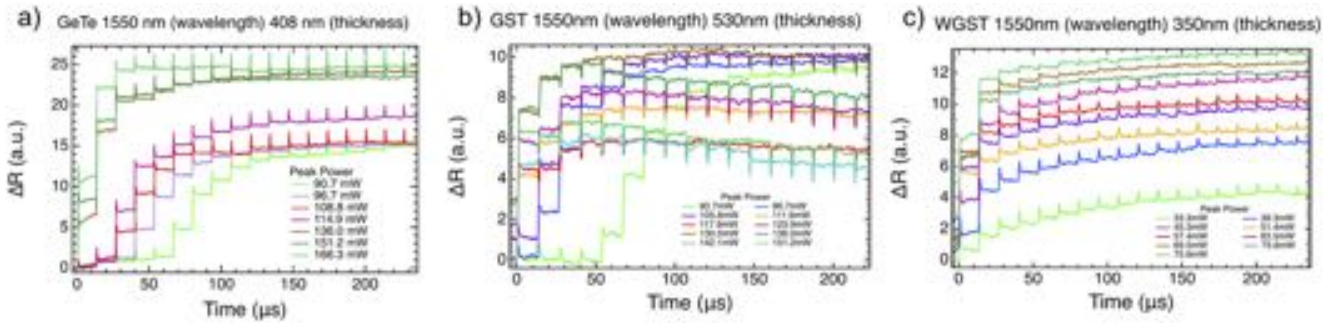

FIG. 5. Multipulse response of (a) GeTe, (b) GST, and (c) W-GST for 1550 nm excitation with thicker films.

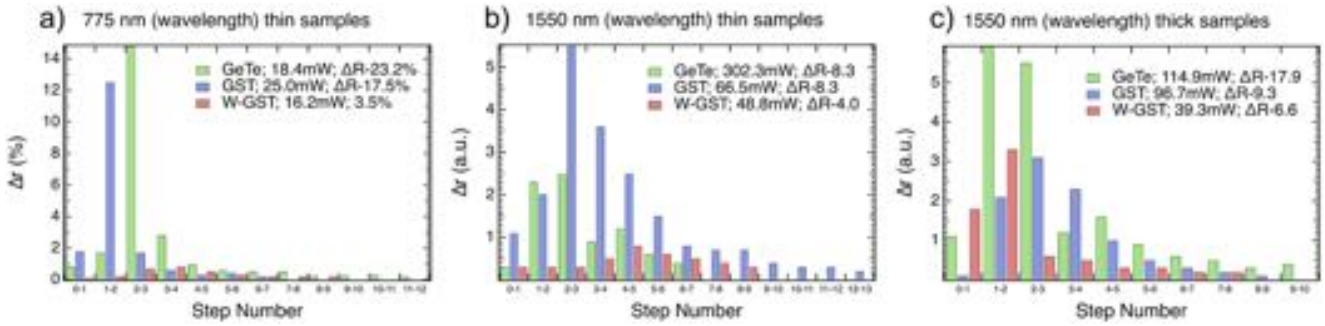

FIG. 6. Summary of data showing the linearity in step size between subsequent intermediate levels during multipulse excitation for (a) 775 nm wavelength on the thin samples, (b) 1550 nm wavelength on the thin samples, and (c) 1550 nm wavelength on the thicker samples. Δr is the distance between reflectivities at each level. The first number in the legend is the peak power used for the maximum number of levels, and the second is the reflection contrast between the lowest and highest levels, with the 1550 nm measurements being in arbitrary units due to the balanced measurement.

wavelengths. We also see a larger ΔR with GeTe than we see in the other materials. Another interesting thing to notice is the fact that GST actually loses a dynamic range going from the 174 nm thick sample to the 530 nm thick sample. This is due to a thin film effect. The change in the reflective dynamic range between fully amorphous and crystallized films for the thin sample is more than double the range of the thicker sample. The higher number of steps available is due to the interaction at the interface of the GST and silicon; the silicon pulls the heat out of GST and allows for a smaller volume to be switched at once. In thicker GST, there is nowhere for the heat to go, and it stays locally and switches to a larger volume. Even with thicker GeTe, the excitation pulse penetrates fully through the material and reaches the silicon, giving a larger volume available for change and increasing the dynamic range. W-GST has a higher thermal conductivity and therefore allows for a faster and more efficient spread of the crystallization, giving an inherently larger crystallization area and a larger dynamic range while not gaining in the number of levels available.

Finally, Fig. 6 shows a summary of the data gained from all three datasets. The figure makes clear the differences between the linearity in level spacing, powers for the maximum number of available levels, and ΔR for each material. At 775 and 1550 nm excitation on the thin samples, it can be seen that W-GST is much more linear in its switching, which for certain applications may be the most important aspect; however, more levels are available in GeTe at 775 nm or GST at 1550 nm. Each material has its own benefits for specific applications.

IV. CONCLUSION

In conclusion, we have shown the differences in crystallization dynamics for three different phase change materials. We investigated GeTe, GST, and W-GST and compared their pros and cons for application in free-space multilevel phase change devices. We identified peak power ranges for crystallization of the materials and gave examples of applications where the differing behaviors would be beneficial. We discovered that by reducing the spot size of the pump laser, we lost access to as many levels as seen in our previous work and recognized a benefit to optimizing the thickness of the sample to take advantage of the interface between the materials for extending the number of levels available. This work adds to the catalog of materials under study for optical PCMs and will serve as a part of the building blocks of a material library for future devices.

ACKNOWLEDGMENTS

This research was supported by the National Science Foundation (NSF) (Grant No. NSF-ECCS-1710273) and the Defense Associated Graduate Student Innovators (DAGSI) (Grant No. RY18-22).

J.R.H. acknowledges support from the Air Force Office of Scientific Research (Program Manager Dr. Gernot Pomrenke) under Award No. FA9550-20RYCOR059.

DATA AVAILABILITY

The data that support the findings of this study are available from the corresponding author upon reasonable request.

REFERENCES

[1]G. A. Sevison, S. Farzinazar, J. A. Burrow, C. Perez, H. Kwon, J. Lee, M. Asheghi, K. E. Goodson, A. Sarangan, J. R. Hendrickson, and I. Agha, "Phase change dynamics and two-dimensional 4-bit memory in $Ge_2Sb_2Te_5$ via telecom-band encoding," ACS Photonics **7**, 480–487 (2020).

[2]K. Jiang, Y. Lu, Z. Li, M. Wang, X. Shen, G. Wang, S. Song, and Z. Song, "GeTe/Sb_4Te films: A candidate for multilevel phase change memory," Mater. Sci. Eng., B **231**, 81–85 (2018).

[3]J. Feldmann, M. Stegmaier, N. Gruhler, C. Rios, C. D. Wright, H. Bhaskharan, and W. H. P. Pernice, "All-optical signal processing using phase-change nanophotonics," in *2017 19th International Conference on Transparent Optical Networks (ICTON)* (IEEE, 2017), pp. 1–3.

[4]P. Guo, A. M. Sarangan, and I. Agha, "A review of germanium-antimony-telluride phase change materials for non-volatile memories and optical modulators," Appl. Sci. **9**, 530 (2019).

[5]J. Feldmann, M. Stegmaier, N. Gruhler, C. Ríos, H. Bhaskaran, C. D. Wright, and W. H. P. Pernice, "Calculating with light using a chip-scale all-optical abacus," Nat. Commun. **8**, 1256 (2017).

[6]S. Abdollahramezani, O. Hemmatyar, H. Taghinejad, A. Krasnok, Y. Kiarashinejad, M. Zandehshahvar, A. Alú, and A. Adibi, "Tunable nanophotonics enabled by chalcogenide phase-change materials," Nanophotonics **9**, 1189–1241 (2020); arXiv:2001.06335.

[7]M. Wuttig, H. Bhaskaran, and T. Taubner, "Phase-change materials for non-volatile photonic applications," Nat. Photonics **11**, 465–476 (2017).

[8]P. I. Trofimov, I. G. Bessonova, P. I. Lazarenko, D. A. Kirilenko, N. A. Bert, S. A. Kozyukhin, and I. S. Sinev, "Rewritable and tunable laser-induced optical gratings in phase-change material films," ACS Appl. Mater. Interfaces **13**, 32031–32036 (2021).

[9]A. Karvounis, B. Gholipour, K. F. MacDonald, and N. I. Zheludev, "All-dielectric phase-change reconfigurable metasurface," Appl. Phys. Lett. **109**, 051103 (2016); arXiv:1604.01330.

[10]M. N. Julian, C. Williams, S. Borg, S. Bartram, and H. J. Kim, "Reversible optical tuning of GeSbTe phase-change metasurface spectral filters for mid-wave infrared imaging," Optica **7**, 746 (2020).

[11]P. Guo, J. A. Burrow, G. A. Sevison, A. Sood, M. Asheghi, J. R. Hendrickson, K. E. Goodson, I. Agha, and A. Sarangan, "Improving the performance of $Ge_2Sb_2Te_5$ materials via nickel doping: Towards RF-compatible phase-change devices," Appl. Phys. Lett. **113**, 171903 (2018).

[12]P. Guo, J. A. Burrow, G. A. Sevison, H. Kwon, C. Perez, J. R. Hendrickson, E. M. Smith, M. Asheghi, K. E. Goodson, I. Agha, and A. M. Sarangan, "Tungsten-doped $Ge_2Sb_2Te_5$ phase change material for high-speed optical switching devices," Appl. Phys. Lett. **116**, 131901 (2020).

[13]Y. Zhang, J. Li, J. B. Chou, Z. Fang, A. Yadav, H. Lin, Q. Du, Z. Han, Y. Huang, H. Zheng, T. Gu, V. Liberman, and K. Richardson, "Broadband transparent optical phase change materials," in *Conference on Lasers and Electro-Optics (CLEO) 2017* (OSA, 2017), pp. 5–6.

[14]W. Jian, "Nonvolatile and ultra-low-loss reconfigurable mode (De) multiplexer/switch using triple-waveguide coupler with $Ge_2Sb_2Se_4Te_1$ phase change material," Sci. Rep. **8**, 15946 (2018).

[15]L. Jiang, Y. Zhang, and J. Yang, "Enhancing phase change memory lifetime through fine-grained current regulation and voltage upscaling," in *IEEE/ACM International Symposium on Low Power Electronics and Design (ISLPED)* (IEEE, 2011), pp. 127–132.

[16]X. Sun, A. Lotnyk, M. Ehrhardt, J. W. Gerlach, and B. Rauschenbach, "Realization of multilevel states in phase-change thin films by fast laser pulse irradiation," Adv. Opt. Mater. **5**, 1700169 (2017).

[17]B.-S. Lee, R. M. Shelby, S. Raoux, C. T. Retter, G. W. Burr, S. N. Bogle, K. Darmawikarta, S. G. Bishop, and J. R. Abelson, "Nanoscale nuclei in phase change materials: Origin of different crystallization mechanisms of $Ge_2Sb_2Te_5$ and AgInSbTe," J. Appl. Phys. **115**, 063506 (2014).

[18]X. Li, N. Youngblood, C. D. Wright, W. Pernice, and H. Bhaskaran, "Non-volatile silicon photonic memory with more than 4-bit per cell capability," arXiv:1904.12740 (2019).

[19]M. Joshi, W. Zhang, and T. Li, "Mercury: A fast and energy-efficient multi-level cell based phase change memory system," in *Proceedings-International Symposium on High-Performance Computer Architecture* (IEEE, 2011), pp. 345–356.

[20]Y. Lai, B. Qiao, J. Feng, Y. Ling, L. Lai, Y. Lin, T. G. Tang, B. Cai, and B. Chen, "Nitrogen-doped $Ge_2Sb_2Te_5$ films for nonvolatile memory," J. Electron. Mater. **34**, 176–181 (2005).

[21]A. Gyanathan and Y.-C. Yeo, "Multi-level phase change memory devices with $Ge_2Sb_2Te_5$ layers separated by a thermal insulating Ta_2O_5 barrier layer," J. Appl. Phys. **110**, 124517 (2011).

[22]S. Abdollahramezani, O. Hemmatyar, M. Taghinejad, H. Taghinejad, A. Krasnok, A. A. Eftekhar, C. Teichrib, S. Deshmukh, M. El-Sayed, E. Pop, M. Wuttig, A. Alu, W. Cai, and A. Adibi, "Electrically driven programmable phase-change meta-switch reaching 80% efficiency," arXiv:2104.10381 (2021).

[23]Y. Zhang, C. Fowler, J. Liang, B. Azhar, M. Y. Shalaginov, S. Deckoff-Jones, S. An, J. B. Chou, C. M. Roberts, V. Liberman, M. Kang, C. Ríos, K. A. Richardson, C. Rivero-Baleine, T. Gu, H. Zhang, and J. Hu, "Electrically reconfigurable non-volatile metasurface using low-loss optical phase-change material," Nat. Nanotechnol. **16**, 661–666 (2021); arXiv:2008.06659.

[24]Y. Wang, P. Landreman, D. Schoen, K. Okabe, A. Marshall, U. Celano, H.-S. P. Wong, J. Park, and M. L. Brongersma, "Electrical tuning of phase-change antennas and metasurfaces," Nat. Nanotechnol. **16**, 667–672 (2021); arXiv:2008.12903.

[25]T. Cao, G. Zheng, S. Wang, and C. Wei, "Ultrafast beam steering using gradient Au-$Ge_2Sb_2Te_5$-Au plasmonic resonators," Opt. Express **23**, 18029 (2015).

[26]G. Rodriguez-Hernandez, P. Hosseini, C. Ríos, C. D. Wright, and H. Bhaskaran, "Mixed-mode electro-optical operation of $Ge_2Sb_2Te_5$ nanoscale crossbar devices," Adv. Electron. Mater. **3**, 1700079 (2017).

[27]G. C. Sosso, G. Miceli, S. Caravati, and M. Bernasconi, "Neural network interatomic potential for the phase change material GeTe," Phys. Rev. B **85**, 174103 (2012).

[28]A. Fantini, L. Perniola, M. Armand, J. F. Nodin, V. Sousa, A. Persico, J. Cluzel, C. Jahan, S. Maitrejean, S. Lhostis, A. Roule, C. Dressler, G. Reimbold, B. De Salvo, P. Mazoyer, D. Bensahel, and F. Boulanger, "Comparative assessment of GST and GeTe materials for application to embedded phase-change memory devices," in *2009 IEEE International Memory Workshop* (IEEE, 2009), pp. 1–2.

[29]L. Chau, J. G. Ho, X. Lan, G. Altvater, R. M. Young, N. El-hinnawy, D. Nichols, J. Volakis, and N. Ghalichechian, "Optically controlled GeTe phase change switch and its applications in reconfigurable antenna arrays," Proc. SPIE **9479**, 947905 (2015).

[30]W. Gawelda, J. Siegel, C. N. Afonso, V. Plausinaitiene, A. Abrutis, and C. Wiemer, "Dynamics of laser-induced phase switching in GeTe films," J. Appl. Phys. **109**, 123102 (2011).

[31]M. Jafari and M. Rais-Zadeh, "An ultra-high contrast optical modulator with 30 dB isolation at 1.55 μm with 25 THz bandwidth," Proc. SPIE **10382**, 1038211 (2017).

[32]C. Rios, M. Stegmaier, Z. Cheng, N. Youngblood, C. D. Wright, W. H. P. Pernice, and H. Bhaskaran, "Controlled switching of phase-change materials by evanescent-field coupling in integrated photonics [Invited]," Opt. Mater. Express **8**, 2455 (2018).

[33]A. Kusiak, J.-L. Battaglia, P. Noé, V. Sousa, and F. Fillot, "Thermal conductivity of carbon doped GeTe thin films in amorphous and crystalline state measured by modulated photo thermal radiometry," J. Phys.: Conf. Ser. **745**, 032104 (2016).